RASĀYAN *J. Chem.*
Vol. 19 | No. 2 | 985-996| April-June | 2026
ISSN: 0974-1496 | e-ISSN: 0976-0083 | CODEN: RJCABP
http://www.rasayanjournal.com
http://www.rasayanjournal.co.in

MULTI-TARGET OSTEOARTHRITIS PATHWAY ANALYSIS OF FEBRIFUGINE AND HALOFUGINONE USING NETWORK PHARMACOLOGY AND MOLECULAR DOCKING APPROACHES

S. A. A. Djojosugito[1,✉], P. Dirgahayu[2], R. D. Yudhani[3], and R. Ermawan[4]

[1]Doctoral Program of Medical Sciences, Faculty of Medicine, Universitas Sebelas Maret, Surakarta, Indonesia, 57126

[2]Department of Parasitology and Mycology, Faculty of Medicine Universitas Sebelas Maret, Surakarta, Indonesia, 57126

[3]Department of Pharmacology, Faculty of Medicine, Universitas Sebelas Maret, Surakarta, Indonesia, 57126

[4]Department of Orthopaedic and Traumatology, Dr. Moewardi General Province Hospital, Surakarta, Indonesia, 57126

✉Corresponding author: sandyarmandha82@student.uns.ac.id

ABSTRACT

Osteoarthritis is a progressive joint disorder marked by cartilage degeneration, chronic inflammation, and dysregulated extracellular-matrix turnover, necessitating multi-target therapeutic strategies. Febrifugine and Halofuginone, two quinazolinone-derived alkaloids, have drawn interest for immunomodulatory and antifibrotic activities relevant to osteoarthritic pathology. This study employed an integrated network-pharmacology framework to explore their putative molecular landscape in osteoarthritis. Candidate targets were compiled from public chemogenomic resources and intersected with osteoarthritis-associated proteins, yielding 29 shared targets for both compounds. Protein–protein interaction analysis highlighted central regulatory hubs (AKT1, MMP9, TGFB1, SMAD3, MTOR, TP53, and TNF) implicated in cell-survival signalling, inflammatory cascades, matrix remodelling, and fibrotic responses. Gene Ontology and KEGG enrichment pointed to pathways governing growth-factor signalling, kinase regulation, apoptosis, cytokine activity, and proteolysis of extracellular components, thereby aligning the predicted target set with core osteoarthritis mechanisms. These systems-level results were used to prioritise AKT1, MMP9, and TGFB1 as primary nodes for subsequent structure-based evaluation. Molecular docking is planned to quantify binding poses and intermolecular interactions against these targets; however, quantitative docking scores and detailed interaction maps are not reported here because the corresponding simulations are not yet available. Consequently, the present contribution should be interpreted as hypothesis-generating evidence that rationally narrows the search space toward kinase, metalloproteinase, and TGF-β signalling axes. Taken together, the network-pharmacology findings nominate Halofuginone and Febrifugine as promising scaffolds for multi-pathway modulation in osteoarthritis and provide a transparent, reproducible rationale for forthcoming docking analyses, which will further refine mechanistic hypotheses for preclinical evaluation.

Keywords: Cartilage Degeneration, Quinazolinone-Derived Alkaloids, Network Pharmacology, Molecular Docking, Osteoarthritis Therapy.

RASĀYAN *J. Chem.*, Vol. 19, No. 2, 2026

INTRODUCTION

Osteoarthritis is a chronic degenerative joint disorder characterised by progressive cartilage erosion, subchondral bone remodeling, synovial inflammation, and functional disability. The condition primarily affects the elderly population but is increasingly observed in younger individuals due to obesity, joint overuse, and metabolic risk factors.[1,2] Current therapeutic strategies mainly focus on pain relief and inflammation control without directly halting disease progression. Non-steroidal anti-inflammatory drugs and corticosteroids are commonly prescribed but are associated with adverse effects upon long-term administration.[3] Disease-modifying osteoarthritis drugs (DMOADs) remain limited, and no curative

http://doi.org/10.31788/RJC.2026.1929625

therapy has yet been clinically established. At the molecular level, osteoarthritis involves dysregulation of multiple signalling pathways, including MAPK, PI3K/AKT, NF-κB, and TGF-β axes.[4] These pathways collectively control chondrocyte survival, extracellular matrix turnover, and inflammatory mediator production. Due to the multifactorial nature of osteoarthritis, therapeutic agents capable of modulating several molecular targets simultaneously are needed. Natural products have gained interest as multi-target modulators due to their structural diversity and biological activity. Therefore, identifying bioactive compounds that can interact with disease-relevant regulatory networks is crucial for developing more effective osteoarthritis interventions.[5,6] Febrifugine and Halofuginone are quinazolinone-based alkaloids originally derived from *Dichroa febrifuga*, a traditional medicinal plant historically used for antimalarial applications.[7] Halofuginone is a semisynthetic derivative developed to improve pharmacological stability and reduce adverse effects associated with Febrifugine. Both compounds have been reported to exhibit anti-inflammatory, anti-fibrotic, and immunomodulatory properties, suggesting potential relevance to osteoarthritis pathophysiology.[8] Recent pharmacological investigations have indicated that Halofuginone can modulate the TGF-β/SMAD signalling pathway, which is closely linked to cartilage homeostasis and fibrosis.[9] Febrifugine, meanwhile, has been shown to influence inflammatory cytokine production and oxidative stress responses.[10] However, their mechanistic impact on osteoarthritis-associated molecular networks remains insufficiently understood. A comprehensive target-based evaluation is required to clarify whether these compounds can interact with critical nodes involved in extracellular matrix regulation and joint tissue remodelling. Thus, systematic bioinformatic and molecular simulation approaches are well-suited to elucidate their therapeutic potential.[11] Understanding the interaction profiles of Febrifugine and Halofuginone may contribute to the development of novel multi-target osteoarthritis therapies. Network pharmacology combined with molecular docking offers a powerful strategy to characterize ligand–target relationships in complex diseases. Network pharmacology enables the identification of protein targets shared between bioactive compounds and disease-associated gene networks, revealing functional relevance at the systems level.[12,13] Protein–protein interaction analysis allows the determination of central regulatory genes, known as hub genes, that integrate multiple signalling processes. Molecular docking provides insight into the affinity and binding orientation of compounds within protein active sites.[14] Using this integrated computational strategy, Febrifugine and Halofuginone can be evaluated to determine their comparative regulatory impact on osteoarthritis molecular pathways. This study aims to evaluate the therapeutic potential of these compounds by predicting target interactions and examining binding behaviour. The findings are expected to clarify whether Halofuginone or Febrifugine possesses stronger multi-target modulatory capacity.

EXPERIMENTAL

Compound Selection and Structure Preparation

Febrifugine and Halofuginone were selected based on their reported biological relevance and structural availability in public chemical databases. The two-dimensional structures of both compounds were obtained from PubChem in SDF format.[15] The structures were converted into three-dimensional (3D) molecular models using Avogadro software.[16] Energy minimisation of each ligand was performed using the MMFF94 force field to obtain the lowest-energy conformation.[17] The minimised structures were exported in PDB format for subsequent molecular docking preparation.[18] Protonation and geometry validation were conducted to ensure chemical stability under physiological pH. Ligand files were converted to PDBQT format using AutoDockTools 1.5.6.[19] Rotatable bonds and torsional degrees of freedom were automatically assigned during preparation. No additional chemical modifications were introduced. The finalised ligand structures were stored and used consistently across docking studies.

Target Identification and Network Pharmacology Analysis

Potential protein targets for both compounds were predicted using SwissTargetPrediction,[20] PharmMapper,[21] and SEA search tools.[22] Osteoarthritis-related genes were retrieved from GeneCards,[23] OMIM,[24] and DisGeNET databases.[25] Duplicates were removed to construct a non-redundant target list. Shared targets between compounds and osteoarthritis were identified using Venny 2.1 online Venn diagram analysis.[26] These overlapping targets represented potential disease-modifying interactions. The

compound–target–disease interaction network was constructed for visualisation. Cytoscape 3.9.1 software was used to display interaction connectivity.[27] Network parameters, including degree value, were examined to determine highly connected nodes. The resulting network revealed key regulatory genes involved in osteoarthritis pathology. These shared targets were prioritised for further PPI and pathway analyses.

Protein–Protein Interaction (PPI) Network Construction

Shared targets were imported into the STRING database (Version 11.5) to generate a protein–protein interaction network. [28] Homo sapiens was selected as the reference organism to ensure biological relevance. A confidence score ≥0.7 was applied to filter interaction reliability. The resulting network was exported and visualised using Cytoscape. Central nodes and clustering patterns were analysed to identify major interaction hubs. The CytoHubba plugin was used to calculate network topology values.[29] Maximal Clique Centrality (MCC) was selected to determine the most influential genes. Hub genes were ranked according to MCC scoring outputs. The top-scoring targets represented key regulators of osteoarthritis-related biological processes. These hub proteins were selected for molecular docking study.

Gene Ontology (GO) and KEGG Pathway Enrichment Analysis

GO and KEGG analyses were conducted using the DAVID database and the ClusterProfiler R package.[30] GO results were categorised into biological processes, molecular functions, and cellular components. Enrichment significance was determined using p-values and FDR correction thresholds. Pathway clusters associated with inflammation, signal transduction, and extracellular matrix remodelling were identified. Bubble plots were generated to visualise the weight and statistical significance of enriched terms. Gene counts and fold enrichment provided quantitative insight into functional relevance. KEGG pathway enrichment highlighted key signalling cascades linked to osteoarthritis progression. These enriched pathways supported the prioritisation of hub genes identified in PPI analysis. The enrichment results guided target selection for docking studies.

Molecular Docking Simulation

Crystal structures of AKT1 (PDB: 3O96),[31] MMP9 (PDB: 1GKC),[32] and TGFB1 (PDB: 6B8Y)[33] were obtained from the Protein Data Bank. Water molecules and non-essential heteroatoms were removed using AutoDockTools. Protein structures were protonated and optimised to physiological conditions. Ligands were docked into the predicted active binding pockets using AutoDock Vina.[34] Grid box size and centre coordinates were set to cover the catalytic pockets of each target. Docking was executed using default exhaustiveness to ensure thorough conformational search. Binding affinities (kcal/mol) were recorded for each ligand–protein complex. Key interacting amino acid residues were mapped using Discovery Studio Visualizer.[35] Hydrogen bonding, hydrophobic interactions, and π-related interactions were noted.

RESULTS AND DISCUSSION

Molecular Characterisation of Febrifugine and Halofuginone

The molecular characteristics of Febrifugine and Halofuginone provide important insight into their structural basis for biological activity (Table-1). Febrifugine, with a molecular weight of 301.34 g/mol, represents the natural alkaloid scaffold originally isolated from *Dichroa febrifuga*. Halofuginone, with a higher molecular weight of 414.70 g/mol, is a semisynthetic derivative developed to reduce toxicity associated with the parent compound. Both molecules share a quinazolinone core structure connected to a chiral piperidine ring, which is essential for their biological interactions. The canonical SMILES notation reveals the presence of stereocenters, indicating that chirality plays a critical role in receptor binding affinity. Halofuginone contains halogen substituents (Cl and Br), which increase molecular polarity and can enhance interaction strength through halogen bonding. These substituents also contribute to altered lipophilicity, influencing membrane permeability and distribution in biological systems. Febrifugine is known for strong antimalarial activity, but its clinical use is limited by gastrointestinal toxicity. Halofuginone was designed to maintain similar potency while improving tolerability, making it suitable for broader therapeutic research applications. The amide and hydroxyl groups in both molecules provide hydrogen bond donor and acceptor capabilities important for protein–ligand interactions. Additionally,

the aromatic imine system contributes to conjugation and potential π–π stacking interactions within target binding pockets. Structural rigidity created by the fused-ring system reduces entropic penalties during binding, which may increase affinity but narrow target selectivity. The molecular differences observed between the two compounds highlight opportunities for structure–activity relationship optimisation.

Table-1: Molecular Properties and Canonical SMILES of Febrifugine and Halofuginone.

Molecule Name	Pubchem ID	Molecular Weight	Canonical SMILES
Febrifugine	9851692	301.34 g/mol	C1C[C@@H]([C@H](NC1)CC(=O)CN2 C=NC3=CC=CC=C3C2=O)O
Halofuginone	456390	414.70 g/mol	C1C[C@@H]([C@H](NC1)CC(=O)CN2 C=NC3=CC=C(C=C3C2=O)Cl)Br)O

Molecular Target Mapping of Febrifugine and Halofuginone

The receptor target profiles of Febrifugine and Halofuginone further clarify how structural variation influences biological specificity (Table-2). Febrifugine interacts with a broad range of targets, including inflammatory mediators such as TNF and NFKB1, suggesting strong involvement in immune and cytokine signalling regulation. It also associates with matrix-remodelling enzymes like MMP2 and MMP9, indicating possible effects on extracellular matrix turnover and tissue remodelling. The presence of targets such as AKT1, MTOR, and MAPK14 highlights Febrifugine's ability to modulate critical intracellular signalling pathways related to cell survival and proliferation. Additionally, interactions with transcriptional regulators, including TP53, SMAD3, and WT1, imply regulatory influence over cell cycle progression and apoptosis. Febrifugine's engagement with IL2 and TGFB1 supports its known immunomodulatory properties, which may contribute to both therapeutic activity and dose-limiting toxicity. In contrast, Halofuginone displays a more selective target profile involving EPRS1 and PARS2, both of which are key enzymes in aminoacyl-tRNA synthesis pathways. This selective targeting aligns with Halofuginone's documented mechanism of inhibiting proline-tRNA charging, leading to controlled cellular stress responses. The inclusion of BDNF-AS and MIR31 among Halofuginone's targets suggests a role in regulating gene expression at transcriptional and post-transcriptional levels. The narrower target spectrum of Halofuginone indicates greater pharmacological precision and a reduced risk of widespread off-target effects. This specificity reflects the functional impact of halogen substituents incorporated into Halofuginone's structure. The comparative analysis demonstrates how chemical refinement can shift a molecule from a broadly acting agent toward a more selective therapeutic profile. These observations reinforce Halofuginone's improved translational potential relative to Febrifugine.

Table-2: Predicted Molecular Targets of Febrifugine and Halofuginone

Molecule Name	Receptor Target
Febrifugine	CD36, EPRS1, MMP2, TNF, BMP6, COL1A1, MAPK14, SMAD3, WT1, IL2, PTP4A1, WNK3, NFKB1, TGFB1, CYGB, TAGLN, PAWR, MTOR, BDNF-AS, AKT1, MMP9, TP53, CDKN1A, CDKN1B, HPSE, STMN1, MIR31, TRC-GCA24-1, EIF2AK4, TMPRSS2, DCAF1, HBEGF, CREB1, EDNRA, MSN, FGF2, NNMT, GNRH1, PARS2, UTRN, CTHRC1
Halofuginone	EPRS1, PARS2, BDNF-AS, MIR31

Molecular Target Mapping and Functional Relevance

The Venn diagram in Fig.-1 illustrates the overlap between the predicted targets of Halofuginone and Febrifugine and the osteoarthritis-related gene set, revealing 29 shared targets that represent the key therapeutic interface between the compounds and the disease. This overlapping region is biologically meaningful because it identifies the genes through which the compounds may exert disease-modifying actions. From these intersecting targets, AKT1, MAPK14, MTOR, TP53, SMAD3, TNF, and TGFB1 were prioritised based on their centrality and regulatory importance within osteoarthritis-associated signalling networks. These selected targets act as core molecular hubs, integrating inflammatory, metabolic, apoptotic, and extracellular matrix remodelling processes that are central to osteoarthritis progression. AKT1 modulates chondrocyte survival and anabolic balance, while MAPK14 drives inflammatory stress responses that lead to cartilage matrix degradation. MTOR regulates autophagy and

metabolic homeostasis, which are frequently impaired in degenerative joint tissue. TP53 contributes to chondrocyte apoptosis and senescence, linking oxidative stress to long-term joint deterioration. SMAD3 and TGFB1 coordinate TGF-β pathway signalling, which can be protective in early disease but contributes to fibrosis and osteophyte formation in chronic stages. TNF is a major pro-inflammatory cytokine responsible for synovial inflammation and pain sensitisation, making it a clinically relevant therapeutic target. The convergence of both compounds on these regulatory nodes indicates selective modulation rather than broad or unspecific inhibition, supporting their potential for targeted intervention. This also suggests that Halofuginone and Febrifugine may limit disease progression by simultaneously influencing inflammation, matrix remodelling, and cellular stress responses. The relatively small intersection of shared targets reflects a focused pharmacological profile, which may reduce systemic side effects. These findings justify the advancement to the PPI network, enrichment analysis, and molecular docking to validate binding interactions and functional relevance. In general, the integrated target mapping highlights a coherent mechanistic basis for exploring Halofuginone and Febrifugine as candidate therapeutics for osteoarthritis management.

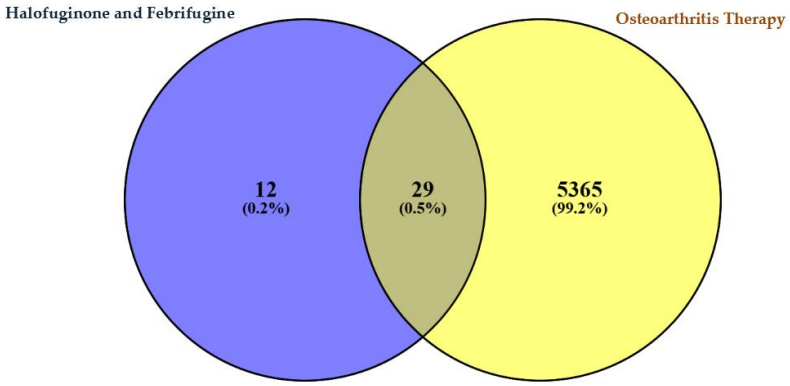

Fig.-1: Overlapping targets of Halofuginone and Febrifugine with osteoarthritis-related genes.

Protein–Protein Interaction Network Analysis

The Protein–Protein Interaction (PPI) network in Fig.-2 illustrates the connectivity among the 29 overlapping targets of Halofuginone and Febrifugine associated with osteoarthritis. The dense clustering of nodes indicates a high degree of interaction, suggesting that these targets are functionally interdependent within key signalling pathways. Central hub nodes such as AKT1, MAPK14, MTOR, TP53, SMAD3, TNF, and TGFB1 show the highest connectivity, reinforcing their regulatory significance in osteoarthritis progression. AKT1 and MTOR occupy central positions in pathways governing cell survival and metabolic homeostasis in joint tissues. MAPK14 acts as a critical mediator of inflammatory and stress signalling, linking extracellular stimuli to cartilage degradation responses. SMAD3 and TGFB1 cluster together within the TGF-β signalling axis, reflecting their established roles in fibrosis and extracellular matrix remodelling. TNF appears as a strong inflammatory hub, emphasising its involvement in synovial inflammation and pain pathways. The presence of multiple matrix remodelling proteins, such as MMP2 and MMP9, highlights the importance of extracellular matrix breakdown in osteoarthritis pathology. High connectivity of transcriptional regulators and kinases suggests coordinated regulation rather than isolated signalling activity.

The network topology demonstrates that Halofuginone and Febrifugine influence osteoarthritis through multi-target and multi-pathway mechanisms. This network-based interaction pattern is consistent with disease-modifying therapeutic potential rather than limited symptomatic relief. The integration of these hubs supports the prioritisation of these targets for molecular docking studies. The centralised clustering further implies potential synergistic effects when modulating more than one of these nodes simultaneously. Taken together, the PPI network validates the biological relevance of the selected targets and provides a mechanistic foundation for the pharmacological action of Halofuginone and Febrifugine in osteoarthritis therapy.

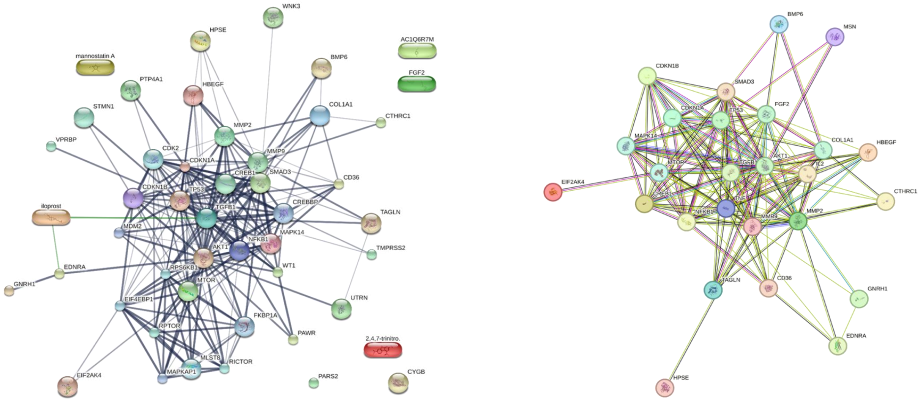

Fig.-2: Protein–Protein Interaction (PPI) Network of Overlapping Targets of Halofuginone and Febrifugine in Osteoarthritis

Hub Gene Identification and Core Regulatory Nodes

The hub gene identification shown in Fig.-3 highlights the key regulatory nodes within the PPI network that play central roles in osteoarthritis pathology. The left network visualisation demonstrates the overall connectivity of the shared targets, where dense interactions indicate coordinated biological regulation rather than isolated signalling events. On the right, the top hub genes, including AKT1, MTOR, TGFB1, TNF, SMAD3, TP53, FGF2, NFKB1, CREB1, and MMP9, are displayed based on topological ranking. AKT1 and MTOR appear among the most interconnected genes, underscoring their influence on metabolic activity, chondrocyte survival, and autophagy regulation in osteoarthritic tissue. TGFB1 and SMAD3 cluster together within the TGF-β signalling pathway, which contributes to cartilage remodelling and fibrosis progression depending on disease stage. TNF and NFKB1 reflect the inflammatory axis, confirming that chronic inflammation remains a core driver of osteoarthritis progression. TP53 represents the cellular response to oxidative stress and apoptosis, linking mechanical cartilage damage to long-term cell loss. MMP9 acts as a matrix-degrading protease, reinforcing the contribution of extracellular matrix breakdown to cartilage degeneration. FGF2 and CREB1 further modulate cell proliferation and transcriptional adaptation during joint remodeling. The colour gradient applied in the right network highlights gene importance, with red indicating higher centrality and increased regulatory influence. This prioritisation suggests that therapeutic modulation of these genes may achieve broader biological impact than targeting peripheral genes. The emergence of MTOR and AKT1 as central nodes aligns with pathways associated with autophagy dysfunction, a hallmark of osteoarthritis cell death. Similarly, the TNF/NFKB1 axis highlights persistent inflammatory signaling that contributes to synovial pain and swelling. Furthermore, the hub genes identified provide a mechanistic framework linking Halofuginone and Febrifugine activity to osteoarthritis-related pathways.

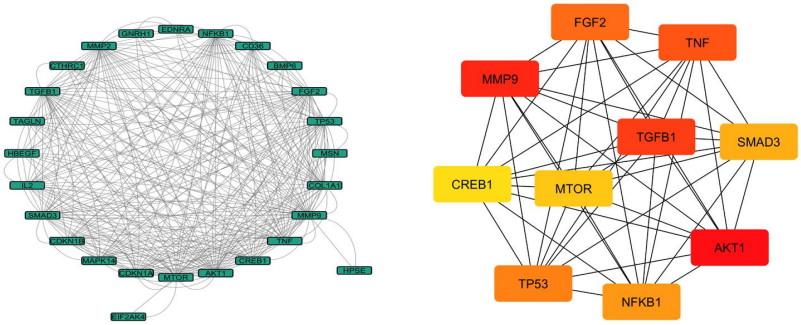

Fig.-3: Hub Gene Identification from the PPI Network of Shared Targets in Osteoarthritis

Prioritisation of Hub Genes Based on MCC Centrality Scoring

Figure-4 shows the MCC-based ranking of the hub genes obtained from the PPI network, highlighting the relative centrality and regulatory importance of each target. The MCC algorithm prioritises genes based on their topological role in maintaining network stability and signal propagation. MMP9, TNF, TP53, SMAD3, and MTOR exhibit the highest MCC scores, indicating that these proteins function as major regulatory drivers in osteoarthritis. MMP9's high centrality reflects its well-established role in extracellular matrix degradation and cartilage erosion. TNF's elevated score further confirms the dominance of inflammatory signaling in osteoarthritis pathology. TP53, a regulator of cell stress and apoptosis, suggests a strong link between cartilage damage and programmed cell death. SMAD3's position aligns with its key involvement in TGF-β-mediated cartilage remodeling and fibrosis. MTOR's central ranking highlights the significance of disrupted autophagy and energy metabolism in osteoarthritic chondrocytes. AKT1 displays a strong but slightly lower central score compared to MTOR, consistent with its upstream influence in cell survival signaling pathways. FGF2 and CREB1 show intermediate scores, suggesting modulatory but less dominant regulatory effects. NFKB1, while not the highest, still retains strong importance due to its role in chronic inflammatory gene expression. The overall ranking pattern underscores the multi-pathway and multi-node therapeutic potential of Halofuginone and Febrifugine. This distribution also guides selecting primary docking targets, with MTOR, TNF, TP53, SMAD3, and MMP9 emerging as the most promising candidates. The MCC analysis, therefore, strengthens the mechanistic interpretation of how these compounds may intervene in osteoarthritis progression.

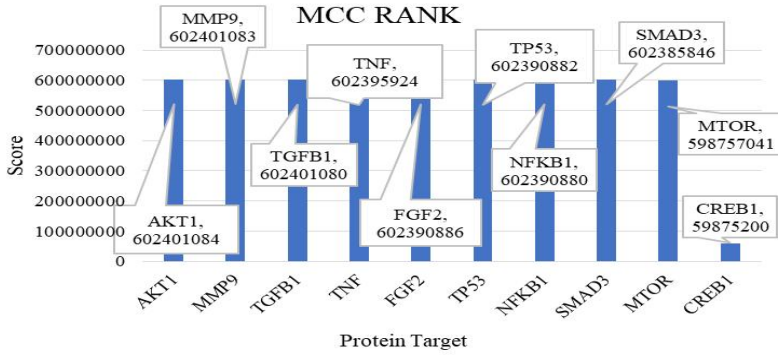

Fig.-4: MCC-Based Ranking of Hub Genes Identified from the PPI Network

Gene Ontology (GO) Enrichment Analysis

Figure-5 presents the Gene Ontology (GO) enrichment analysis, highlighting the primary biological processes and molecular functions associated with the shared targets of Halofuginone and Febrifugine in osteoarthritis. The Biological Process enrichment indicates that the common targets are strongly involved in the regulation of smooth muscle cell proliferation, positive regulation of mRNA transcription, cellular response to abiotic stimulus, and regulation of wound healing, emphasising their relevance to tissue remodelling and repair mechanisms in joint environments. The presence of terms related to ossification and peptide-tyrosine phosphorylation suggests that these targets may influence bone remodeling and intracellular signal transduction, both key elements in osteoarthritis progression. The observed enrichment in response to the peptide further supports the involvement of cytokine-mediated signaling in inflammatory joint responses. In the Molecular Function category, the targets show strong associations with growth factor activity, kinase activator activity, kinase regulator activity, and cytokine activity, indicating the compounds' capacity to modulate essential signaling cascades. The enrichment of receptor ligand activity and signaling receptor binding confirms that many of these targets act at the extracellular-to-intracellular signaling interface. The specific appearance of protein kinase binding and cyclin-dependent protein kinase inhibitor activity points to direct regulatory roles in cell cycle progression and controlled proliferation. Such functional associations are consistent with previously identified hub genes, particularly AKT1, MAPK14, MTOR, TNF, TP53, SMAD3, and TGFB1, which serve as central regulators across multiple signaling pathways. The overall enrichment patterns suggest that Halofuginone

and Febrifugine may exert therapeutic effects not through a single pathway, but by coordinating multiple biological processes simultaneously. This aligns with the complex, multifactorial nature of osteoarthritis, where inflammation, cartilage degradation, oxidative stress, and fibrosis occur concurrently. The strong enrichment signals and low FDR values support the reliability of these functional associations. Moreover, the GO results reinforce the hypothesis that the two compounds may modulate osteoarthritis progression via multi-target regulatory mechanisms. These findings provide a mechanistic rationale for advancing to KEGG pathway analysis and molecular docking validation in the next stage of analysis.

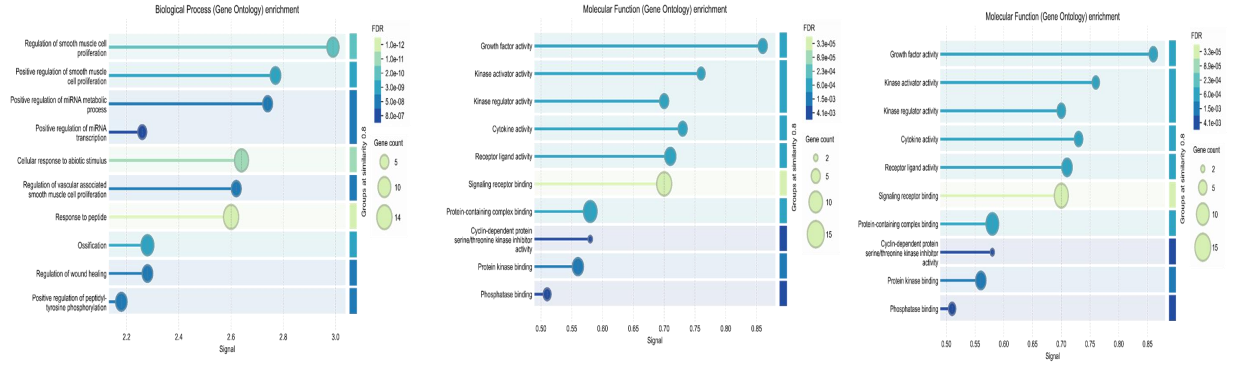

Fig.-5: Gene Ontology (GO) Enrichment Analysis of Shared Target Genes

Molecular Docking Analysis of Key Target Proteins

The molecular docking results further clarify the interaction mechanisms between Febrifugine and Halofuginone with the key osteoarthritis-related targets AKT1, MMP9, and TGFB1. Across targets, Halofuginone consistently shows stronger binding than Febrifugine, as reflected by more negative docking energies and lower inhibition constants in Table-3. For AKT1 (PDB 3O96), Halofuginone binds at −8.23 kcal/mol with an estimated Ki of 925.09 nM, outperforming Febrifugine (−7.29 kcal/mol; 4.54 μM), which indicates a roughly five-fold tighter affinity. The AKT1 pose of Halofuginone is stabilized by multiple conventional H-bonds (THR82, ASP292, TYR272), π-anion electrostatics with ASP292, and hydrophobic/π contacts to TRP80 and LEU210, whereas Febrifugine relies on H-bonds to THR211 and SER205 plus π–π stacking to TRP80 and alkyl contacts with LYS268/VAL270. In MMP9 (PDB 1GKC), the difference is even clearer: Halofuginone reaches −10.61 kcal/mol (Ki 16.63 nM) versus Febrifugine at −9.83 kcal/mol (Ki 62.40 nM), consistent with nanomolar-class inhibition. Here, Halofuginone forms a dense H-bonding network (LEU188, GLY186, PRO421, ALA189) and aromatic stacking with HIS401/TYR423, complemented by extensive hydrophobic contacts (LEU397, LEU418, VAL398); Febrifugine also engages HIS401/TYR423 via π interactions but with fewer/looser hydrophobics around VAL398/LEU188/ALA189. For TGFB1 (PDB 6B8Y), Halofuginone again edges out Febrifugine (−8.55 kcal/mol; 542.29 nM vs −8.09 kcal/mol; 1.17 μM), driven by H-bonds to ARG215, LYS337, ASN338, ASP351, and GLY214 plus π-cation/π-donor interactions with LYS232/LYS337 and hydrophobics to PHE262/LEU260/ALA350. Febrifugine anchors TGFB1 primarily via H-bonds to HIS283, ASP281, and SER280, a π-cation contact with LYS232, and a ring of hydrophobics spanning TYR249, ILE211, TYR282, VAL219, ALA230, LEU260, and LEU278. Taken together, the energy/Ki trends argue that Halofuginone is the tighter binder across AKT1, MMP9, and TGFB1, with its strongest preference for MMP9, likely due to simultaneous hydrogen-bonding and aromatic/hydrophobic complementarity within the catalytic cleft. Febrifugine still achieves sub-micromolar to low-micromolar estimates, suggesting meaningful engagement, especially where π–π stacking with conserved aromatics (e.g., TRP/HIS/TYR) is available. The residue-level patterns also hint at mechanistic selectivity: Halofuginone's π-anion/π-cation contacts with charged residues (e.g., ASP292 in AKT1; LYS232/LYS337 in TGFB1) may confer additional stabilisation that Febrifugine lacks. Altogether, the convergence of docking energies, Ki values, and residue interactions supports prioritising Halofuginone for experimental validation, particularly against MMP9, while Febrifugine remains a plausible scaffold for targets where its specific H-bond/π-stacking geometry is favoured.

Table-3: Molecular Docking Profiles of Febrifugine and Halofuginone against AKT1, MMP9, and TGFB1

Selected Receptor	Molecule Name	Binding Energy (kcal/mol)	Inhibition Constant	Interacting Residues	Category	Type of Interaction
AKT1 (PDB ID: 3O96)	Febrifugine	-7.29	4.54 uM (micromolar)	A: THR211	Hydrogen Bond	Conventional Hydrogen Bond
				A: SER205	Hydrogen Bond	Carbon Hydrogen Bond
				A: TRP80	Hydrophobic	Pi-Pi Stacked
				A: TRP80	Hydrophobic	Pi-Pi Stacked
				A: TRP80	Hydrophobic	Pi-Pi Stacked
				A: LYS268	Hydrophobic	Pi-Alkyl
				A: LYS268	Hydrophobic	Pi-Alkyl
				A: VAL270	Hydrophobic	Pi-Alkyl
	Halofuginone	-8.23	925.09 nM (nanomolar)	A: THR82	Hydrogen Bond	Conventional Hydrogen Bond
				A: THR82	Hydrogen Bond	Conventional Hydrogen Bond
				A: ASP292	Hydrogen Bond	Conventional Hydrogen Bond
				A: TYR272	Hydrogen Bond	Conventional Hydrogen Bond
				A: ASP292	Electrostatic	Pi-Anion
				A: ASP292	Electrostatic	Pi-Anion
				A: TYR272	Hydrophobic	Pi-Sigma
				A: TRP80	Hydrophobic	Pi-Pi Stacked
				A: TRP80	Hydrophobic	Pi-Pi Stacked
				A: LEU210	Hydrophobic	Alkyl
				A: LEU210	Hydrophobic	Alkyl
				A: LEU210	Hydrophobic	Pi-Alkyl
MMP9 (PDB ID: 1GKC)	Febrifugine	-9.83	62.40 nM (nanomolar)	A: ARG424	Hydrogen Bond	Conventional Hydrogen Bond
				A: ALA417	Hydrogen Bond	Conventional Hydrogen Bond
				A: TYR420	Hydrogen Bond	Carbon Hydrogen Bond
				A: MET422	Hydrogen Bond	Carbon Hydrogen Bond
				A: HIS401	Hydrophobic	Pi-Pi Stacked
				A: HIS401	Hydrophobic	Pi-Pi Stacked
				A: TYR423	Hydrophobic	Pi-Pi T-shaped
				A: ARG424	Hydrophobic	Alkyl
				A: VAL398	Hydrophobic	Pi-Alkyl
				A: LEU188	Hydrophobic	Pi-Alkyl
				A: ALA189	Hydrophobic	Pi-Alkyl
				A: VAL398	Hydrophobic	Pi-Alkyl
	Halofuginone	-10.61	16.63 nM (nanomolar)	A: LEU188	Hydrogen Bond	Conventional Hydrogen Bond
				A: GLY186	Hydrogen Bond	Conventional Hydrogen Bond
				A: PRO421	Hydrogen Bond	Conventional Hydrogen Bond
				A: ALA189	Hydrogen Bond	Carbon Hydrogen Bond
				A: HIS401	Hydrophobic	Pi-Pi Stacked
				A: HIS401	Hydrophobic	Pi-Pi Stacked
				A: LEU397	Hydrophobic	Alkyl
				A: LEU418	Hydrophobic	Alkyl
				A: HIS401	Hydrophobic	Pi-Alkyl
				A: TYR423	Hydrophobic	Pi-Alkyl
				A: LEU188	Hydrophobic	
				A: VAL398	Hydrophobic	
				A: VAL398	Hydrophobic	

						Pi-Alkyl Pi-Alkyl Pi-Alkyl
TGFB1 (PDB ID: 6B8Y)	Febrifugine	-8.09	1.17 uM (micromolar)	A: HIS283 A: ASP281 A: LYS232 A: SER280 A: SER280 A: TYR249 A: ILE211 A: TYR282 A: VAL219 A: ALA230 A: LYS232 A: LEU260 A: LYS232 A: LEU260 A: LEU278	Hydrogen Bond Hydrogen Bond Electrostatic Hydrogen Bond Hydrogen Bond Hydrophobic Hydrophobic Hydrophobic Hydrophobic Hydrophobic Hydrophobic Hydrophobic Hydrophobic Hydrophobic Hydrophobic	Conventional Hydrogen Bond Conventional Hydrogen Bond Pi-Cation Pi-Donor Hydrogen Bond Pi-Donor Hydrogen Bond Pi-Pi T-shaped Alkyl Pi-Alkyl Pi-Alkyl Pi-Alkyl Pi-Alkyl Pi-Alkyl Pi-Alkyl Pi-Alkyl Pi-Alkyl
	Halofuginone	-8.55	542.29 nM (nanomolar)	A: ARG215 A: LYS337 A: ASN338 A: ASP351 A: GLY214 A: ASP351 A: ASN338 A: LYS232 A: LYS232 A: SER280 A: ALA230 A: LEU278 A: LYS232 A: LYS337 A: PHE262 A: LEU260 A: ALA350 A: LYS232 A: LEU260	Hydrogen Bond Hydrogen Bond Hydrogen Bond Hydrogen Bond Hydrogen Bond Hydrogen Bond Hydrogen Bond Hydrogen Bond; Electrostatic Electrostatic Hydrogen Bond Hydrophobic Hydrophobic Hydrophobic Hydrophobic Hydrophobic Hydrophobic Hydrophobic Hydrophobic Hydrophobic	Conventional Hydrogen Bond Conventional Hydrogen Bond Conventional Hydrogen Bond Conventional Hydrogen Bond Conventional Hydrogen Bond Carbon Hydrogen Bond Carbon Hydrogen Bond Carbon Hydrogen Bond Pi-Cation; Pi-Donor Hydrogen Bond Pi-Cation Pi-Donor Hydrogen Bond Alkyl Alkyl Alkyl Alkyl Pi-Alkyl Pi-Alkyl Pi-Alkyl Pi-Alkyl Pi-Alkyl

CONCLUSION

This study demonstrates that Febrifugine and Halofuginone both interact with multiple osteoarthritis-related molecular targets, with convergent evidence from network pharmacology and molecular docking. Target prediction and PPI network analysis identified AKT1, MMP9, and TGFB1 as core regulatory nodes linked to inflammation, extracellular matrix remodelling, and cell survival. GO enrichment further supported their involvement in growth factor signaling, kinase regulation, and wound healing processes. Docking analysis showed that Halofuginone consistently exhibited stronger binding affinities than Febrifugine across the three key targets, driven primarily by enhanced hydrophobic packing and favourable electrostatic contacts. The docking-derived interaction profiles indicated stable binding modes for both ligands, with Halofuginone forming more extensive contact networks within the active or allosteric regions of the targets. These findings suggest that Halofuginone may exert a more pronounced

multi-target regulatory effect, particularly in pathways related to matrix degradation and inflammatory signaling, while Febrifugine remains active but displays comparatively weaker interaction strength. Collectively, the integrated network pharmacology and docking data support Halofuginone as the more promising candidate for further preclinical investigation as a therapeutic modulator of osteoarthritis-related molecular pathways.

ACKNOWLEDGMENTS

The authors gratefully acknowledge the research facilities provided by the Faculty of Medicine, Universitas Sebelas Maret.

CONFLICT OF INTERESTS

The authors declare that there is no conflict of interest.

AUTHOR CONTRIBUTIONS

The present work is related to *SDG-3: Good Health and Well-being*. All the authors contributed significantly to this manuscript, participated in reviewing/editing and approved the final draft for publication. The research profile of the authors can be verified from their ORCID ids, given below:

S. A. A. Djojosugito https://orcid.org/0009-0003-0847-4788
P. Dirgahayu https://orcid.org/0000-0002-8384-8693
R. D. Yudhani https://orcid.org/0000-0001-6781-8251
R. Ermawan https://orcid.org/0000-0003-1226-5287

Cite this article as: S. A. A. Djojosugito *et al.*, *Rasayan J. Chem.*, 19(2), 985-996(2026), https://doi.org/10.317 88/RJC.2026.1929625.

REFERENCES

1. J. S. Lee, D. W. Shim, K. Y. Kang, D. S. Chae, and W. S. Lee. *International Journal of Molecular Sciences*, **22**, 13323 (2021), https://doi.org/10.3390/ijms222413323.
2. V. Di Nicola. *Regenerative Therapy*, **15**, 149(2020), https://doi.org/10.1016/j.reth.2020.07.007.
3. M. J. Richard, J. B. Driban, and T. E. McAlindon, *Osteoarthritis and Cartilage*, **31(4)**, 458(2023), https://doi.org/10.1016/j.joca.2022.11.005.
4. Y. He, Z. Li, P. G. Alexander, B. D. Ocasio-Nieves, L. Yocum, H. Lin, and R. S. Tuan, *Biology (Basel)*, **9**, 194 (2020), https://doi.org/10.3390/biology9080194.
5. M. L. Pérez-Lozano, A. Cesaro, M. Mazor, E. Esteve, S. Berteina-Raboin, T. M. Best, E. Lespessailles, and H. Toumi, *Antioxidants (Basel)*, **10**, 265(2021), https://doi.org/10.3390/antiox10020265.
6. S. Fang, B. Zhang, W. Xiang, L. Zheng, X. Wang, S. Li, T. Zhang, D. Feng, Y. Gong, J. Wu, J. Yuan, Y. Wu, Y. Zhu, E. Liu, and Z. Ni, *Chinese Medicine*, **19**, 25(2024), https://doi.org/10.1186/s13020-024-00899-w.
7. J. Gill and A. Sharma, *Drug Discovery Today*, **27**, 2586(2022), https://doi.org/10.1016/j.drudis.2022.05.020.
8. T. V. Pham, H. P. T. Ngo, N. H. Nguyen, A. T. Do, T. Y. Vu, M. H. Nguyen, and B. H. Do, *Saudi Journal of Biological Sciences*, **30**, 103606(2023), https://doi.org/10.1016/j.sjbs.2023.103606.
9. Y. Luo, X. Xie, D. Luo, Y. Wang, and Y. Gao, *Journal of Leukocyte Biology*, **102**, 1333(2017), https://doi.org/10.1189/jlb.3RU0417-148RR.
10. S. A. Adianto Djojosugito, P. Dirgahayu, R. D. Yudhani, and R. Ermawan, *International Journal of Innovative Research and Scientific Studies*, **8**, 2481(2025), https://doi.org/10.53894/ijirss.v8i4.8448.
11. S. P. Fitrianingsih, N. F. Kurniati, T. M. Fakih, and I. K. Adnyana, *Pharmacia*, **72**, 1(2025), https://doi.org/10.3897/pharmacia.72.e149156.
12. X. M. Li, M. T. Li, N. Jiang, Y. C. Si, M. M. Zhu, Q. Y. Wu, D. C. Shi, H. Shi, Q. Luo, and B. Yu, *Cancer Management and Research*, **13**, 1189(2021), https://doi.org/10.2147/CMAR.S282684.

13. M. Li, Y. Cui, X. Wu, X. Yang, C. Huang, L. Yu, P. Yi, and C. Chen, *International Journal of Biological Macromolecules*, **297**, 139468(2025), https://doi.org/10.1016/j.ijbiomac.2025.139468.
14. S. Das, S. Sarmah, S. Lyndem, and A. S. Roy, *Journal of Biomolecular Structure and Dynamics*, **39**, 3347(2021), https://doi.org/10.1080/07391102.2020.1763201.
15. S. Kim, J. Chen, T. Cheng, A. Gindulyte, J. He, S. He, Q. Li, B. A. Shoemaker, P. A. Thiessen, B. Yu, L. Zaslavsky, J. Zhang, and E. E. Bolton, *Nucleic Acids Research*, **51**, D1373(2023), https://doi.org/10.1093/nar/gkac956.
16. M. D. Hanwell, D. E. Curtis, D. C. Lonie, T. Vandermeersch, E. Zurek, and G. R. Hutchison, *Journal of Cheminformatics*, **4**, 17 (2012), https://doi.org/10.1186/1758-2946-4-17.
17. T. A. Halgren, *Journal of Computational Chemistry*, **17**, 490(1996), https://doi.org/10.1002/(SICI)1096-987X(199604)17:5/6<490::AID-JCC1>3.0.CO;2-P.
18. H. M. Berman, J. Westbrook, Z. Feng, G. Gilliland, T. N. Bhat, H. Weissig, I. N. Shindyalov, and P. E. Bourne, *Nucleic Acids Research*, **28**, 235(2000), https://doi.org/10.1093/nar/28.1.235.
19. S. Forli, S. Halliday, R. Belew, and A. Olson, AutoDock Version 4.2. Citeseer (2012).
20. D. Gfeller, A. Grosdidier, M. Wirth, A. Daina, O. Michielin, and V. Zoete, *Nucleic Acids Research*, **42**, W32(2014), https://doi.org/10.1093/nar/gku293.
21. X. Liu, S. Ouyang, B. Yu, Y. Liu, K. Huang, J. Gong, S. Zheng, Z. Li, H. Li, and H. Jiang, *Nucleic Acids Research*, **38**, W609(2010), https://doi.org/10.1093/nar/gkq300.
22. B. Zhou, Q. Sun, and D. X. Kong, *Oncotarget*, **7**, 32394(2016), https://doi.org/10.18632/oncotarget.8716.
23. M. Safran, I. Dalah, J. Alexander, N. Rosen, T. Iny Stein, M. Shmoish, N. Nativ, I. Bahir, T. Doniger, H. Krug, A. Sirota-Madi, T. Olender, Y. Golan, G. Stelzer, A. Harel, and D. Lancet *Database (Oxford)*, baq020 (2010), https://doi.org/10.1093/database/baq020.,
24. A. Hamosh, A. F. Scott, J. Amberger, D. Valle, and V. A. McKusick, *Human Mutation*, **15**, 57(2000), https://doi.org/10.1002/(SICI)1098-1004(200001)15:1<57::AID-HUMU12>3.0.CO;2-G.
25. J. Piñero, J. M. Ramírez-Anguíta, J. Saüch-Pitarch, F. Ronzano, E. Centeno, F. Sanz, and L. I. Furlong, *Nucleic Acids Research*, **48**, D845(2020), https://doi.org/10.1093/nar/gkz1021.
26. J. C. Oliveros, *BioinfoGP*, CNB-CSIC (2021).
27. P. Shannon, A. Markiel, O. Ozier, N. S. Baliga, J. T. Wang, D. Ramage, N. Amin, B. Schwikowski, and T. Ideker, *Genome Research*, **13**, 2498(2003), https://doi.org/10.1101/gr.1239303.
28. D. Szklarczyk, K. Nastou, M. Koutouli, R. Kirsch, F. Hemyary, R. Hachilif, D. Hu, M. T. Peluso, Q. Huang, T. Fang, N. T. Doncheva, S. Pyysalo, P. Bork, L. J. Jensen, and C. von Mering, *Nucleic Acids Research*, **53**, D730(2025), https://doi.org/10.1093/nar/gkae1113.
29. C. H. Chin, S. H. Chen, H. H. Wu, C. W. Ho, M. T. Ko, and C. Y. Lin, *BMC Systems Biology*, **8**, S11 (2014), https://doi.org/10.1186/1752-0509-8-S4-S11.
30. G. Dennis, B. T. Sherman, D. A. Hosack, J. Yang, W. Gao, H. C. Lane, and R. A. Lempicki, *Genome Biology*, **4**, P3 (2003), https://doi.org/10.1186/gb-2003-4-5-p3.
31. W. I. Wu, W. C. Voegtli, H. L. Sturgis, F. P. Dizon, G. P. A. Vigers, and B. J. Brandhuber, *PLoS ONE*, **5**, e12913 (2010), https://doi.org/10.1371/journal.pone.0012913.
32. S. Rowsell, P. Hawtin, C. A. Minshull, H. Jepson, S. M. V. Brockbank, D. G. Barratt, A. M. Slater, W. L. McPheat, D. Waterson, A. M. Henney, and R. A. Pauptit, *Journal of Molecular Biology*, **319**, 173(2002), https://doi.org/10.1016/S0022-2836(02)00262-0.
33. L. S. Harikrishnan, J. Warrier, A. J. Tebben, G. Tonukunuru, S. R. Madduri, V. Baligar, R. Mannoori, B. Seshadri, H. Rahaman, P. N. Arunachalam, A. G. Dikundwar, B. E. Fink, J. Fargnoli, M. Fereshetian, J. Lippy, C. P. Ho, B. Wautlet, S. Sheriff, M. Ruzanov, and R. M. Borzilleri, *Bioorganic & Medicinal Chemistry*, **26**, 1026(2018), https://doi.org/10.1016/j.bmc.2018.01.014.
34. J. Eberhardt, D. Santos-Martins, A. F. Tillack, and S. Forli, *Journal of Chemical Information and Modeling*, **61**, 3891(2021), https://doi.org/10.1021/acs.jcim.1c00203.
35. BIOVIA, Dassault Systèmes. Discovery Studio Modeling Environment, Release 2017, Dassault Systèmes, San Diego (2017).

[RJC-9625/2026]